Trajectory-based interpretation of Young's experiment, the Arago–Fresnel laws and the Poisson–Arago spot for photons and massive particles

2013 Phys. Scr. 2013 014015

(http://iopscience.iop.org/1402-4896/2013/T153/014015)

Phys. Scr. **T153** (2013) 014015 (5pp) doi:10.1088/0031-8949/2013/T153/014015

Trajectory-based interpretation of Young's experiment, the Arago–Fresnel laws and the Poisson–Arago spot for photons and massive particles

Milena Davidović[1], Ángel S Sanz[2], Mirjana Božić[3], Dušan Arsenović[3] and Dragan Dimić[4]

[1] Faculty of Civil Engineering, University of Belgrade, Bulevar Kralja Aleksandra 73, Belgrade, Serbia
[2] Instituto de Física Fundamental (IFF-CSIC), Serrano 123, E-28006 Madrid, Spain
[3] Institute of Physics, University of Belgrade, Pregrevica 118, Belgrade, Serbia
[4] Faculty of Natural and Mathematical Sciences, University of Niš, Niš, Serbia

E-mail: milena@grf.bg.ac.rs, asanz@iff.csic.es, bozic@ipb.ac.rs, arsenovic@ipb.ac.rs and divladq@hotmail.com

Received 14 September 2012
Accepted for publication 23 October 2012
Published 28 March 2013
Online at stacks.iop.org/PhysScr/T153/014015

Abstract
We present a trajectory-based interpretation of Young's experiment, the Arago–Fresnel laws and the Poisson–Arago spot. This approach is based on the equation of the trajectory associated with the quantum probability current density in the case of massive particles, and the Poynting vector for the electromagnetic field in the case of photons. Both the form and properties of the evaluated photon trajectories are in good agreement with the averaged trajectories of single photons observed recently in Young's experiment by Steinberg's group at the University of Toronto. In the case of the Arago–Fresnel laws for polarized light, the trajectory interpretation presented here differs from interpretations based on the concept of 'which-way' (or 'which-slit') information and quantum erasure. More specifically, the observer's information about the slit that the photons went through is not relevant to the existence of interference; what is relevant is the form of the electromagnetic energy density and its evolution, which will model consequently the distribution of trajectories and their topology. Finally, we also show that the distributions of end points of a large number of evaluated photon trajectories are in agreement with the distributions measured at the screen behind a circular disc, clearly giving rise to the Poisson–Arago spot.

PACS numbers: 03.50.De, 03.65.Ta, 42.25.Hz, 42.50.−p

(Some figures may appear in color only in the online journal)

1. Introduction

Very refined and ingenious interferometers and detectors for electrons [1], neutrons [2–4], atoms [5–7], molecules [7, 8] and photons [9, 10] have been devised to demonstrate that the quantum interference pattern can be built up by means of the accumulation of single detection events. Even before the realization of these experiments, de Broglie [11] and Bohm [12] argued that particles with mass possess simultaneously wave and particle properties, and would move within an interferometer along trajectories determined by the guidance equation

$$\vec{v} = \frac{\mathrm{d}\vec{r}}{\mathrm{d}t} = \frac{\nabla S(\vec{r}, t)}{m}, \tag{1}$$

where $S(\vec{r}, t)$ is the phase of the particle wave function

$$\Psi(\vec{r}, t) = |\Psi(\vec{r}, t)|\, \mathrm{e}^{\mathrm{i}S(\vec{r},t)/\hbar}, \tag{2}$$

which satisfies the time-dependent Schrödinger equation.

Using the method proposed by De Broglie [11] and Bohm [12], Philippidis *et al* [13] plotted the trajectories of massive particles in the double-slit experiment [13], Dewdney [14] showed trajectories for neutrons inside a (neutron) interferometer and Sanz and Miret-Artés [15] explained the Talbot effect for atoms by plotting their associated trajectories behind a diffraction grating.

Motivated by the works of Laukien [16], presented in [17], and Prosser [18], Davidović *et al* [19] explained the emergence of interference patterns in experiments with photons by determining electromagnetic energy (EME) flow lines behind an interference grating. The equation of such EME flow lines reads as

$$\frac{\mathrm{d}\vec{r}}{\mathrm{d}s} = \frac{\vec{S}(\vec{r})}{cU(\vec{r})}, \tag{3}$$

where s denotes a certain arc-length along the corresponding path, $\vec{S}(\vec{r})$ is the real part of the complex-valued Poynting vector

$$\vec{S}(\vec{r}) = \tfrac{1}{2}\mathrm{Re}[\vec{E}(\vec{r}) \times \vec{H}^*(\vec{r})] \tag{4}$$

and $U(\vec{r})$ is the time-averaged EME density

$$U(\vec{r}) = \tfrac{1}{4}\left[\varepsilon_0 \vec{E}(\vec{r}) \cdot \vec{E}^*(\vec{r}) + \mu_0 \vec{H}(\vec{r}) \cdot \vec{H}^*(\vec{r})\right]. \tag{5}$$

Here $\vec{E}(\vec{r})$ and $\vec{H}(\vec{r})$ are, respectively, the spatial parts of the electric and magnetic field vectors, which satisfy Maxwell's equations and have been assumed to be harmonic, i.e.

$$\begin{aligned} \vec{\tilde{H}}(\vec{r}, t) &= \vec{H}(\vec{r})\, \mathrm{e}^{-\mathrm{i}\omega t}, \\ \vec{\tilde{E}}(\vec{r}, t) &= \vec{E}(\vec{r})\, \mathrm{e}^{-\mathrm{i}\omega t}. \end{aligned} \tag{6}$$

Davidović *et al* [19] pointed out that it is useful to write the equation of the Bohmian trajectories for massive particles (1) in terms of the probability current density,

$$\vec{J}(\vec{r}, t) = \frac{\hbar}{2\mathrm{i}m}\left[\Psi \nabla \Psi^* - \Psi^* \nabla \Psi\right], \tag{7}$$

because from the latter form, one can recast the guidance equation (1) as

$$\frac{\mathrm{d}\vec{r}}{\mathrm{d}t} = \frac{\vec{J}(\vec{r}, t)}{|\Psi(\vec{r}, t)|^2}, \tag{8}$$

from which one may conclude that the equation for the EME flow lines and the equation of the Bohmian trajectories for massive particles have the same form. In other words, the Poynting vector in the case of photons plays the same role as the quantum probability current density in the case of particles with a mass.

This analogy is even more apparent in the cases where the spatial parts of the magnetic and electric fields can be expressed in terms of a scalar function that satisfies the Helmholtz equation [19, 20].

Gondran and Gondran [21] explained the appearance of the Poisson–Arago spot behind an illuminated circular disc using EME flow lines. In this way, they showed how such flow lines answer the question about diffraction phenomena presented two centuries ago by the French Academy 'deduce by mathematical induction, the movements of the rays during their crossing near the bodies'.

Recently, average trajectories of single photons in a double-slit experiment were observed experimentally for the first time by Kocsis *et al* [22]. Their result motivated us to apply the method of EME flow lines to numerically evaluate photon trajectories behind the double-slit grating with the same parameters as in the Kocsis *et al* experiment. We show these results in section 2. In section 3, we study how polarizers put behind the slits affect the photon trajectories, thus providing a trajectory interpretation for the Arago–Fresnel laws. By adding orthogonal polarizers behind the slits, Kocsis *et al* could observe average photon trajectories in the presence of orthogonal polarizers and check directly this interpretation. Section 4 is devoted to the trajectory-based interpretation of the Poisson–Arago spot.

2. Electromagnetic energy (EME) flow lines: average photon trajectories in a Young's interferometer

Let us consider a monochromatic electromagnetic wave in vacuum incident onto a two-slit grating located on the XY-plane, at $z = 0$. In order to simplify the treatment, we will assume that the electric and magnetic fields do not depend on the y-coordinate. This assumption is justified when the slits are parallel to the y-axis and their width along the y-axis is much larger than the width along the x-axis. In such a case from Maxwell's equations one obtains two independent sets of equations: one involving the H_x and H_z components of the magnetic field and the E_y component of the electric field (commonly referred to as E-polarization), and another involving E_x, E_z and H_y (H-polarization). As shown in [19], the electric and magnetic fields behind the grating are given by

$$\vec{E}(\vec{r}) = -\frac{\mathrm{i}\beta}{k}\frac{\partial \Psi}{\partial z}\vec{e}_x + \frac{\mathrm{i}\beta}{k}\frac{\partial \Psi}{\partial x}\vec{e}_z + \alpha \Psi \vec{e}_y, \tag{9}$$

$$\vec{H}(\vec{r}) = \frac{\mathrm{i}\alpha}{\omega\mu_0}\frac{\partial \Psi}{\partial z}\vec{e}_x - \frac{\mathrm{i}\alpha}{\omega\mu_0}\frac{\partial \Psi}{\partial x}\vec{e}_z + \frac{k\beta \mathrm{e}^{\mathrm{i}\varphi}}{\omega\mu_0}\Psi \vec{e}_y, \tag{10}$$

where Ψ is a scalar function that satisfies the Helmholtz equation and the boundary conditions at the grating. The solution for Ψ can be written as a Fresnel–Kirchhoff integral,

$$\Psi(x, z) = \sqrt{\frac{k}{2\pi z}}\mathrm{e}^{-\mathrm{i}\pi/4}\,\mathrm{e}^{\mathrm{i}kz}\int_{-\infty}^{+\infty}\psi\left(x', 0^+\right)\mathrm{e}^{\mathrm{i}k(x-x')^2/2z}\,\mathrm{d}x', \tag{11}$$

where $\psi(x', 0^+)$ is the wave function just behind the grating.

We consider a grating with two Gaussian slits [23], so that the wave function just behind the grating is given by

$$\psi(x', 0^+) = \psi_1(x', 0^+) + \psi_2(x', 0^+), \tag{12}$$

where

$$\psi_1(x', 0^+) = (2\sigma_1^2\pi)^{-1/4}\,\mathrm{e}^{-(x'-\mu_1)^2/4\sigma_1^2} w(x' - \mu_1, a_1), \tag{13}$$

$$\psi_2(x', 0^+) = (2\sigma_2^2\pi)^{-1/4}\,e^{-(x'-\mu_2)^2/4\sigma_2^2} w(x' - \mu_2, a_2), \tag{14}$$

and $w(x, a)$ is the window function

$$w(x, a) = \begin{cases} 1, & x \in [-a, a], \\ 0, & x \notin [-a, a]. \end{cases} \tag{15}$$

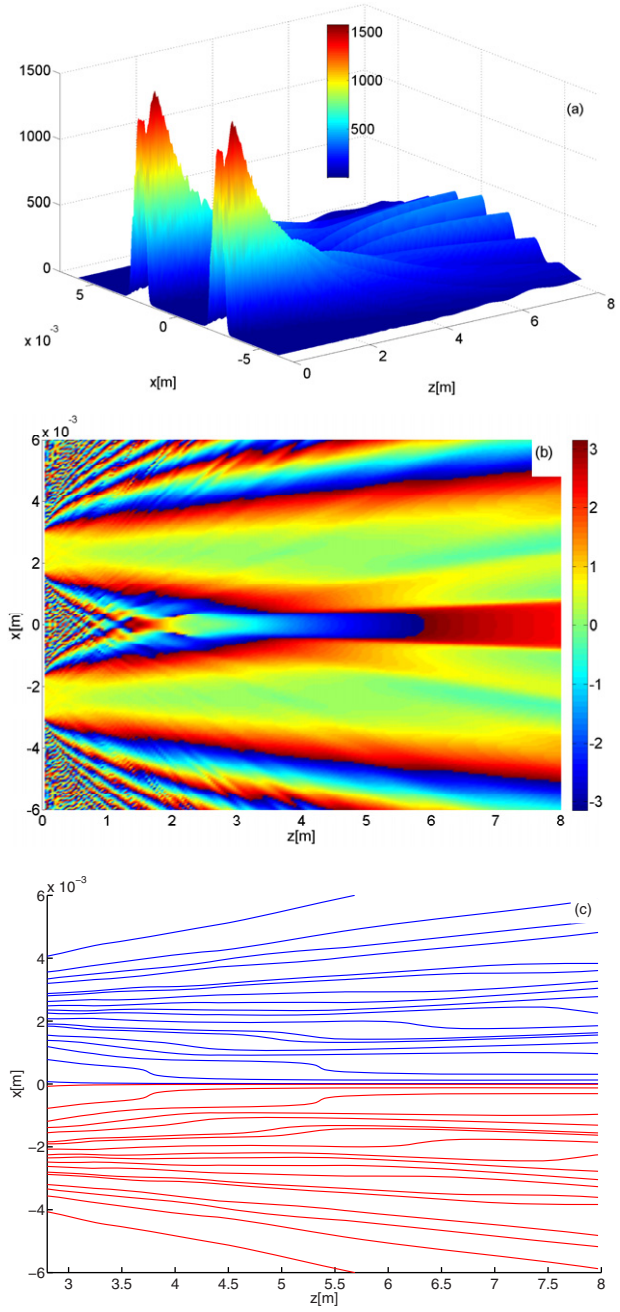

Figure 1. EME density (a), phase of $\Psi(x,\ z)$ (b) and photon trajectories (c) behind a two-slit Gaussian grating. The parameters are chosen as in the experiment carried out by Kocsis *et al*: $\sigma_1 = \sigma_2 = 0.3$ mm, $\mu_1 = -\mu_1 = 2.35$ mm, $a_1 = a_2 = 1.8\sigma_1$ and $\lambda = 943$ nm. Initial polarization is linear. The initial x-coordinates for the trajectories are calculated from (16), where u takes 19 equidistant values within the interval $[0.02,\ 0.98]$.

The EME flow lines (i.e. the average photon trajectories from the experiment carried out by Kocsis *et al*) are obtained from equations (3)–(5) and (9)–(15). In figure 1, 19 photon trajectories per slit are shown. The initial x-coordinates of the flow lines are chosen to be

$$x_s = \mu_i + \sigma_i\, F^{-1}(u)\,, \tag{16}$$

where $i \in \{1,\ 2\}$ is the cardinal number of the slit and $F^{-1}(u)$ is the inverse of the Gaussian cumulative distribution function. If the variable u follows a uniform distribution, then the variable x_s will have a Gaussian distribution with the mean value μ_i and variance σ_i.

Comparing the photon trajectories displayed in figure 1(c) with those experimentally inferred, as shown in figure 3 in [22], we notice very good agreement. The experimental average photon paths were reconstructed after carrying out a weak measurement on the momentum of an ensemble of photons and then a subsequent strong measurement of their position. In figure 2, we compare the experimental data coming from the measurement of the relative weak transverse momentum values, k_x/k, as a function of the transverse coordinate at four different distances from the grating, with our theoretical curves obtained for three different window functions.

Since in our case the light propagates in vacuum, the Poynting vector can be identified with the density of electromagnetic momentum [24], so we have

$$\frac{k_x}{k} = \frac{S_x}{S}. \tag{17}$$

The Fresnel–Kirchhoff integral [17] can be integrated analytically for full Gaussians (for which the parameter of the window function $a \to \infty$), whereas the integration has to be done numerically for truncated Gaussians, as we did here.

3. EME flow-line interpretation of the Arago–Fresnel laws

According to a generalized version of the Arago–Fresnel laws, two beams with the same polarization state interfere with each other just as natural rays do, but no interference pattern will be observable if the two interfering beams are linearly polarized in orthogonal directions or elliptically polarized, with opposite handedness and mutually orthogonal major axes. The most direct way of verifying these laws is by inserting mutually orthogonal polarizers behind the slits of a double-slit grating.

The standard interpretation given to the disappearance of the interference fringes after inserting mutually orthogonal polarizers behind the slits is usually based on the Copenhagen notion of the external observer's knowledge (information) about the path followed by the photon, i.e. the slit traversed by the photon in its way to the detection screen. Sanz *et al* [20] and Božić *et al* [25] challenged this interpretation by explaining the first and second Arago–Fresnel laws considering EME flow lines behind the grating both in the presence and in the absence of polarizers. In both the cases, EME flow lines starting from slit 1 will end up in the side in front of slit 1, whereas those starting from slit 2 will end up in the side in front of slit 2, as also shown in quantum mechanics for matter particles [26]. However, the distribution of these EME flow lines is different in each case. In the absence of polarizers, the distribution shows interference fringes (figure 1(c) and figure 5 in [25]); in the presence of polarizers, the fringes are absent (figure 3 and figure 6 in [25]).

As seen above, the average photon trajectories observed by Kocsis *et al* [22] in the absence of polarizers agree with our EME flow lines—the photon paths presented in figure 1. In order to verify the interpretation of the Arago–Fresnel laws

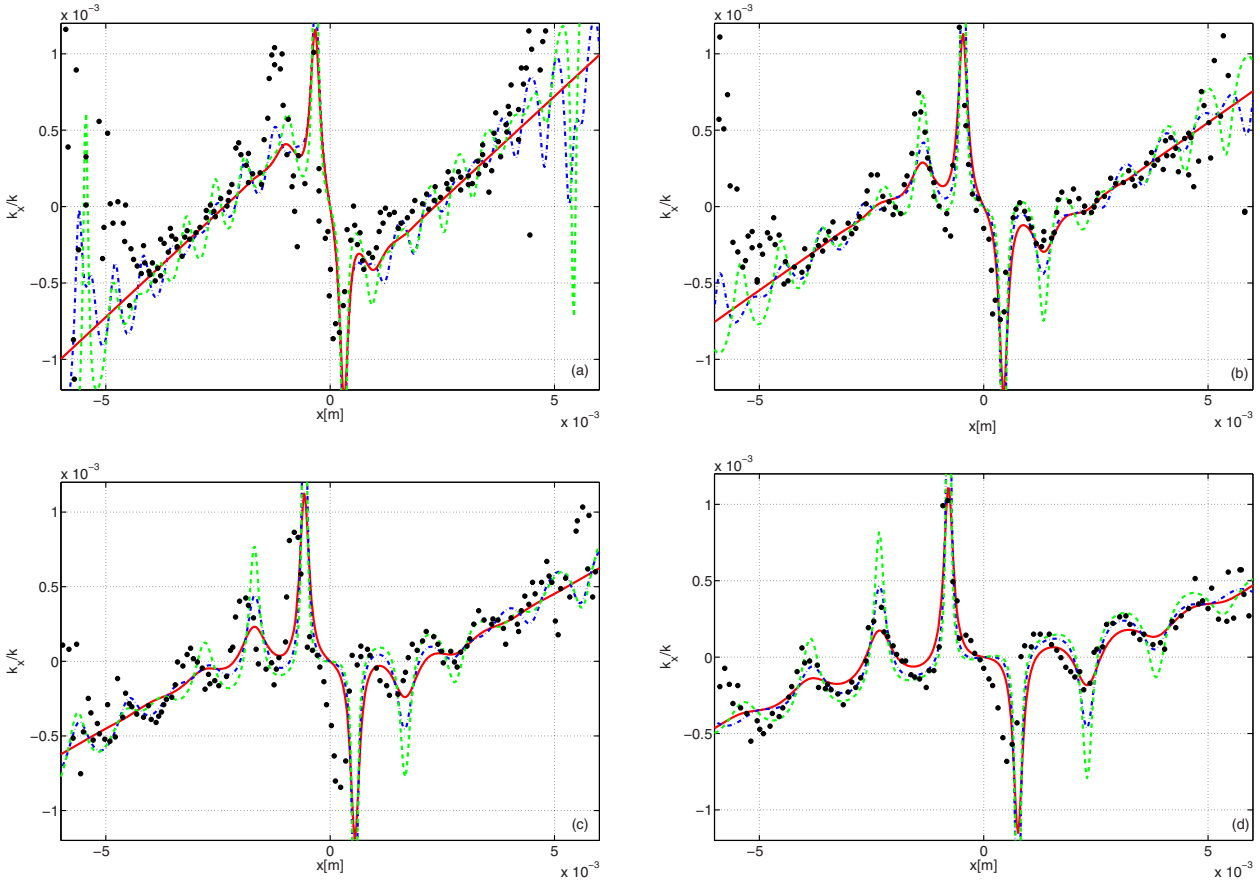

Figure 2. Transverse momentum along the transverse coordinate computed at four distances z from the two slits: (a) $z = 3.2$ m, (b) $z = 4.5$ m, (c) $z = 5.6$ m and (d) $z = 7.7$ m. The red solid line denotes the calculation with full Gaussians, whereas the blue and green lines refer to calculations where the outgoing beams were truncated Gaussians with $a = 1.9\sigma$ and 1.5σ, respectively. For comparison, the experimental data (black circles) are also displayed. Parameters used for the calculation are: $\sigma_1 = 0.307$ mm, $\sigma_2 = 0.301$ mm, $\mu_1 = 2.335$ mm, $\mu_2 = -2.355$ mm, $a_1 = 1.5\sigma_1$, $a_2 = 1.5\sigma_2$ and $\lambda = 943$ nm.

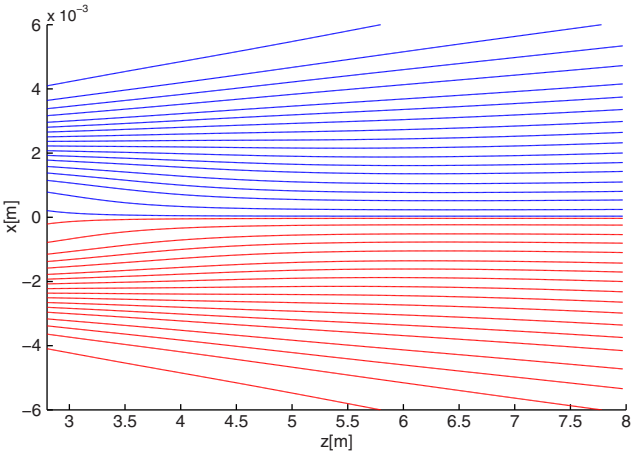

Figure 3. Photon trajectories behind a Gaussian double-slit grating followed by orthogonal polarizers. The parameters are the same as those in figure 1.

based on the EME flow lines, it would be interesting as well as challenging to experimentally determine the average photon paths in a slightly modified experimental setup, by adding orthogonal polarizers behind the slits. In such a case, we expect that the corresponding experimentally inferred photon paths would look like the trajectories presented in figure 3.

4. EME flow-line interpretation of the Poisson–Arago spot

It is well known that the experimental observation of the so-called Poisson–Arago spot[5] by Arago led to the acceptance of Fresnel's wave theory of light and the refutation of Newton's corpuscular theory of light. Now, by numerically evaluating EME flow lines behind a circular opaque disc, Gondran and Gondran [21] found that these lines can reach the bright Poisson–Arago spot that appears at the center of the shadow region generated by such a disc. These authors then argued that for a monochromatic wave in vacuum, the EME flow lines correspond to the diffracted rays of Newton's *Opticks*, thus concluding that after all Fresnel's wave theory may not be in contradiction with the corpuscular interpretation. This result also follows from our evaluation of EME flow lines (figure 4). Statistics of these lines (see figure 5) agrees very well with the corresponding curve of light intensity behind the circular disc [21, 27] determined by taking the square of the field function $\Psi(x, y, z)$, which is given by the Rayleigh–Sommerfeld formula and Babinet's

[5] This phenomenon is commonly known simply as the Poisson spot. However, we have added the name of Arago in order to give him scientific credit, for it was he who provided experimental evidence for this light phenomenon.

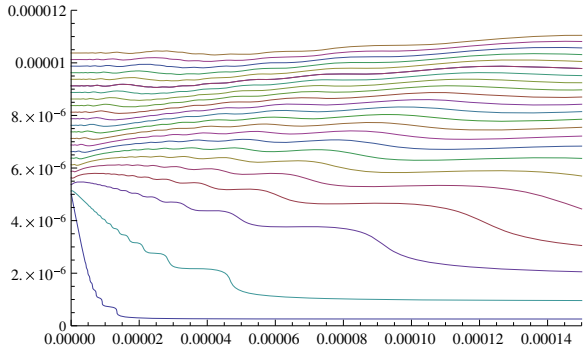

Figure 4. Photon trajectories in the *XZ*-plane behind a circular disc in the *XY*-plane, centered at $x = y = z = 0$ and with radius $R = 5\,\mu$m. The disc is illuminated by a monochromatic light with wavelength $\lambda = 500$ nm. Because of the cylindrical symmetry of the problem, only trajectories having positive initial *x*-coordinate are presented.

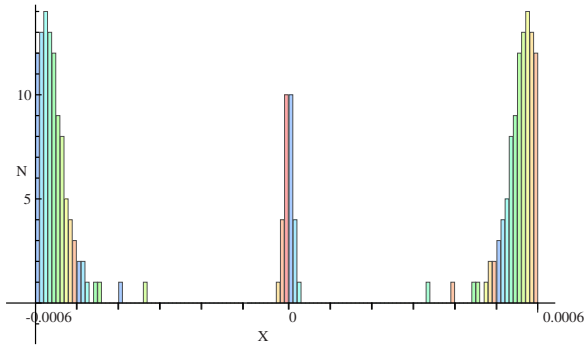

Figure 5. Histogram of the end points of photon trajectories at distance $z = 15$ mm behind a circular disc of radius $R = 0.5$ mm illuminated by monochromatic light with wavelength $\lambda = 500$ nm.

principle [21, 28],

$$\Psi(x, y, z) = \Psi_0 \left(e^{ikz} + \int_S \frac{e^{ikr}}{r} \left(1 - \frac{1}{ikr}\right) \cos\theta \, dx_M \, dy_M \right), \tag{18}$$

where $r = \sqrt{(x - x_M)^2 + (y - y_M)^2 + z^2}$, $\cos\theta = \frac{z}{r}$, $k = \frac{2\pi}{\lambda}$ and integration is taken on the surface of the opaque disc S.

Due to circular symmetry the integration over two variables in (18) may be reduced to the integration over one variable. This simplifies and makes faster the numerical evaluation of the field function and the trajectories. In addition, this simplified formula makes possible the analysis of the dependence of the field function on the longitudinal *z*-coordinate. The details of this study constitute the subject of a forthcoming paper, where we will also present the Bohmian trajectories corresponding to a recent Poisson–Arago spot experiment performed with molecules [29].

Acknowledgment

MD, MB and DA acknowledge support from the Ministry of Science of Serbia under projects OI171005, OI171028 and III45016. ASS acknowledges support from the Ministerio de Economía y Competitividad (Spain) under projects FIS2010-22082 and FIS2011-29596-C02-01, as well as a 'Ramon y Cajal' Research Fellowship.

References

[1] Merli P G, Missiroli G F and Pozzi G 1976 *Am. J. Phys.* **44** 306
[2] Rauch H, Treimer W and Bonse U 1974 *Phys. Lett.* A **47** 369
[3] Rauch H and Werner S 2000 *Neutron Interferometry: Lessons in Experimental Quantum Mechanics* (Oxford: Clarendon)
[4] Klein T 2009 *Europhys. News* **40/6** 24
[5] Keith D W, Ekstrom C R, Turchette Q A and Pritchard D E 1991 *Phys. Rev. Lett.* **66** 2693
[6] Kurtsiefer Ch, Pfau T and Mlynek J 1997 *Nature* **386** 150
[7] Berman P R (ed) 1997 *Atom Interferometry* (New York: Academic)
[8] Juffmann T, Nimmrichter S, Arndt M, Gleiter H and Hornberger K 2012 *Found. Phys.* **42** 98
[9] Parker S 1971 *Am. J. Phys.* **39** 420
Parker S 1972 *Am. J. Phys.* **40** 1003
[10] Dimitrova T L and Weis A 2008 *Am. J. Phys.* **76** 137
[11] de Broglie L 1963 *Etude Critique des Bases de l'Interpretation Actuelle de la Mecanique Ondulatoire* (Paris: Gauthier-Villars)
de Broglie L 1964 *Etude Critique des Bases de l'Interpretation Actuelle de la Mecanique Ondulatoire* (Amsterdam: Elsevier) Engl. transl.
[12] Bohm D 1952 *Phys. Rev.* **85** 166
Bohm D 1952 *Phys. Rev.* **85** 180
[13] Philippidis C, Dewdney D and Hiley B J 1979 *Nuovo Cimento* B **52** 15
[14] Dewdney C 1985 *Phys. Lett.* A **109** 377
[15] Sanz A S and Miret-Artés S 2007 *J. Chem. Phys.* **126** 234106
[16] Laukien G 1952 *Optik* **9** 174
[17] Born M and Wolf E 1999 *Principles of Optics* 7th edn (New York: Wiley)
[18] Prosser R D 1976 *Int. J. Theor. Phys.* **15** 169
Prosser R D 1976 *Int. J. Theor. Phys.* **15** 181
[19] Davidović M, Sanz A S, Arsenović D, Božić M and Miret-Artés S 2009 *Phys. Scr.* **T135** 014009
[20] Sanz A S, Davidović M, Božić M and Miret-Artés S 2010 *Ann. Phys.* **325** 763
[21] Gondran M and Gondran A 2010 *Am. J. Phys.* **78** 598
Gondran M and Gondran A 2009 hal-00416055
[22] Kocsis S, Braverman B, Ravets S, Stevens M J, Mirin R P, Shalm L K and Steinberg A M 2011 *Science* **332** 1170
[23] Feynman R P and Hibbs A 1965 *Quantum Mechanics and Path Integrals* (New York: McGraw-Hill)
[24] Barnett M and Loudon R 2010 *Phil. Trans. R. Soc.* A **368** 927
[25] Božić M, Davidović M, Dimitrova T L, Miret-Artés S, Sanz A S and Weis A 2010 *J. Russ. Laser Res.* **31** 117
[26] Sanz A S and Miret-Artés S 2012 *A Trajectory Description of Quantum Processes: I. Fundamentals* (*Lecture Notes in Physics* vol 850) (Berlin: Springer)
[27] Rinard P M 1976 *Am. J. Phys.* **44** 70
[28] Sommerfeld A 1967 *Optics* vol IV (New York and London: Academic)
[29] Reisinger T, Patel A A, Reingruber H, Fladischer K, Ernst W E, Bracco G, Smith H I and Holst B 2009 *Phys. Rev.* A **79** 053823